



Published in final edited form as:

*Adv Mater.* 2013 June 4; 25(21): 2903–2908. doi:10.1002/adma.201300383.

## Full Range Magnetic Manipulation of Droplets via Surface Energy Traps Enables Complex Bioassays

Yi Zhang and

3400 North Charles Street, Clark 122, Baltimore, Maryland 21218, USA

Prof. Tza-Huei Wang

3400 North Charles Street, Latrobe 108, Baltimore, Maryland 21218, USA

Tza-Huei Wang: thwang@jhu.edu

### Keywords

Droplet microfluidics; Lab-on-a-chip (LOC); magnetic droplet actuation; surface energy trap; wetting

Implementing complex bioanalytical assays on fully integrated and scalable lab-on-a-chip (LOC) devices has great potential in key biomedical applications such as point-of-care diagnostics and high-throughput screening [1–5]. However, there are significant challenges because the current LOC devices mostly rely on continuous flow microfluidics and require multifaceted fluidic architectures, components such as pumps and valves, and an external fluid interface to carry out complex bioassays. To address the challenges of these channel-based, continuous flow systems, there is increasing interest in developing droplet-based microfluidic systems [6–9]. Diverse mechanisms have been used for droplet actuation, including electrowetting [10–14], magnetic force [15–18], photo-actuation [19–21], surface acoustic wave [22], and dielectrophoresis [23]. Of these, electrowetting is most widely used because it is capable of comprehensive fluidic operation including dispensing, splitting, and transport. Nonetheless, such a wide range of fluidic operation by electrowetting requires a closed or two-plate configuration, in which droplets are tightly sandwiched between two substrates patterned with electrodes, resulting in a restricted operating liquid volume (100s nL–1  $\mu$ L) [6, 8]. This small assay volume may be impractical for assays that require large sample volume, such as PCR-based detection of infectious agents due to statistical sampling errors. Furthermore, electrowetting alone is limited to liquid handling, and cannot be used to manipulate the solid materials used in heterogeneous assays. Usually a secondary mechanism, such as magnetic forces or dielectrophoresis, is needed for particle handling [14, 24–28].

In contrast, magnetic actuation uses an external magnetic field to manipulate droplets containing magnetizable particles (MPs). Besides functioning as droplet actuators, MPs also

---

Correspondence to: Tza-Huei Wang, thwang@jhu.edu.

Supporting Information

Supporting Information is available from the Wiley Online Library or from the author.

serve as a solid substrate for molecule absorption and separation. Therefore, magnetic actuation provides a promising approach to implementing bioanalytical assays in open surface droplet microfluidic systems. However, magnetic actuation alone performs only a limited set of simple fluidic operations, thus significantly hindering its applicability in complex assays. For example, liquid dispensing, which is a universal process required for sample aliquoting, serial dilution, and droplet splitting for parallel and multiplexed reactions, has not been achieved on any magnetic droplet platforms.

We have now developed a surface energy traps (SETs)-based magnetic droplet manipulation platform that enables a full range of fluidic operations. A SET is an etched area of high surface energy on a glass substrate coated with a low surface energy Teflon film to assist droplet manipulation (Fig. 1A–C). Similar designs can also be implemented to functionalize Teflon coated surface for molecule and cell adhesion in electrowetting-based microfluidic systems [29–31]. We have developed a rapid single-step process to precisely pattern SETs of varying geometries on the substrate, which enables a unique magnetic droplet microfluidic platform capable of a full range droplet manipulations, including droplet transport, fusion, particle extraction, and liquid dispensing (Fig. 1D–G). The SETs design enables complex assays which could not be achieved by traditional magnetic droplet systems.

## Results and Discussion

SETs are fabricated by etching pre-deposited Teflon AF film (Fig. 1A, B) using O<sub>2</sub> plasma [32]. Polydimethylsiloxane (PDMS) stamp was previously used as the etching stencil [33–36]. We have developed a lithographically defined reusable SU8 shadow mask as stencil. Using the ready-made shadow mask, the patterning process bypasses lithography and consists of only a single step (see “methods and materials” and Fig. S1 in supporting information), which completes in 3 minutes, and the SU8 shadow mask is reusable.

Droplet manipulation was demonstrated on the SETs-enabled magnetic droplet microfluidic platform. The MPs were added to droplets, which had been stained with food dye to aid visualization (Fig. 1D–G). By moving a magnet beneath the substrate, the MPs formed a plug and dragged the orange droplet, travelling freely on the low-energy regions of the Teflon film, and transferring the material to pre-designated locations where the green droplet sat (Fig. 1D and supporting information Video V1). When two droplets were brought into proximity, they fused together, thus mixing their materials and allowing reactions to occur (Fig. 1E and supporting information Video V1).

The extraction of MPs was facilitated by large SETs which immobilized the entire droplet by pinning down the contact line. MPs continued travelling until they broke the surface tension, and separated themselves from the droplet (Fig. 1F and supporting information Video V1). MP extraction is an intricate process, which depends on the interplay between magnetic force, capillary force, and frictional force [37]. The operating conditions, such as droplet volume, MPs amount, and magnet moving speed, require fine-tuning within a narrow range in order to extract MPs [37]. Early work used physical energy barriers to restrict droplet movement and facilitate MPs extraction [17, 38]. On our new platform, the

SETs restrict droplet movement by pinning down its contact line, which is far more efficient.

Our method for droplet splitting, allowing liquid to be dispensed and new droplets to be generated, takes advantage of the fact that small SETs withhold only the minority of the liquid, while majority of the droplet escapes from SETs together with MPs (Fig. 1G and supporting information Video V2). Droplets containing fluorescein were dispensed using SETs of various sizes, and their volumes were estimated based on the fluorescent intensities. We show that the volume of the daughter droplet was determined by the size of the SET (Fig. 1H).

Droplets dispensed by SETs exhibited high uniformity. For droplets generated on the same chip with SETs of the same size, the coefficient of variation (CV) in volume was approximately 3% (supporting information Fig. S2). For droplets dispensed on different chips, the CV was larger, approximately 10%, due to chip-to-chip variation (Fig. 1H). Nonetheless, this method enables the dispensing of sub-microliter volumes on a magnetic droplet microfluidic platform with reasonable accuracy. Its simplicity and accuracy provides a rapid and reliable method of generating droplet microarrays on an open surface droplet platform (Fig. 1I). We were also able to dispense daughter droplets using SETs when they were submerged in mineral oil (supporting information Fig. S2 and supporting information Video V3). This would be a significant advantage because mineral oil is often included in droplet based assays to prevent droplet evaporation during transportation and reactions.

As describe earlier, when the MPs pull a droplet over a SET, one of three phenomena are observed, (i) particle extraction, (ii) droplet dispensing, and (iii) magnet disengagement (Fig. 2A–C). In particle extraction, the entire droplet is immobilized by the SET, while the MPs travel with the magnet and are extracted from the droplet. In droplet dispensing, the SET only holds a small portion of liquid within its boundary, and majority portion of the droplet travels with the MPs, leaving behind a daughter droplet. In magnet disengagement, the SET contains the entire droplet as well as MPs as they disengage from the moving magnet.

To be able to predict which of these three phenomena will occur, we need to understand the governing dynamics. SETs function by immobilizing the liquid through contact line pinning. When MPs are pulled from the SET, they stretch and deform the droplet, leading to the formation of two necking points with around the SET (NP1) and the other around MP plug (NP2) (Fig. 2D). As the MPs continue travelling away from the SET, the radius of curvature at the two necking points gradually decreases until one reaches a negative value, causing breakage at the necking point. Breakage at NP2 results in particle extraction, breakage at NP1 results in droplet dispensing, and either necking point breaks in the case of magnet disengagement. Whether the necking points break and which necking point breaks first depends on the MPs amount, SET size, and droplet volume. Simply speaking, the SET and the MPs engage in a tug-of-war with the droplet until one of the necking points yields.

The phenomenon can be explained by the interaction between four elements: the magnetic force, the surface tension around SET, the capillary forces around the MPs plug and SETs, and the friction imposed on the droplet (Fig. 2D). The magnetic force  $F_m$  along the travel

direction is proportional to the amount of MPs  $M$  [37]. At a constant speed, the friction  $F_{drag}$  is approximately proportional to the base radius of the droplet, or  $V_d^{1/3}$  where  $V_d$  is the volume of the droplet, assuming the droplet is hemispherical [37]. The surface tension  $F_i$  around the SET is proportional to its diameter  $D$ .

The unique interactions of the four elements that produce particle extraction, droplet dispensing, and magnet disengagement, are now described. In particle extraction, NP2 breaks first when  $F_m$  is greater than the combined force of  $F_{drag}$  and  $F_i$ , and greater than the capillary force  $F_{c2}$  at NP2. Under these conditions, the MPs can overcome the surface tension and split from the droplet (Fig. 2D). In droplet dispensing, NP1 breaks first when  $F_m$  exceeds the combined force of  $F_{drag}$  and  $F_i$ , and the capillary force around the SET  $F_{c1}$  is smaller than  $F_i$ . Meanwhile,  $F_m$  is smaller than the capillary force  $F_{c2}$  at NP2 in order for MPs to remain in the droplet. In magnet disengagement,  $F_m$  is smaller than  $F_{c2}$ , and smaller than the combined force of  $F_{drag}$  and  $F_i$ . Similarly, the capillary force  $F_{c1}$  at NP1 is greater than  $F_i$ . As a result, the droplet is immobilized by the SET, and MPs are contained within the droplet, in which case neither the droplet nor the MPs can move with the magnet.

With a fixed droplet volume (Fig. 2A), large SETs stabilize NP1, and hold the droplet in position until NP2 breaks, leading to particle extraction. In comparison, large amount of MPs stabilize NP2, and drag the entire droplet until NP1 breaks. Magnet disengagement is observed with small amounts of MPs, in which case  $F_m$  is too weak for the MPs to either overcome the surface tension or to pull the entire droplet. The effect of droplet volume on SET operation was examined while keeping the SET diameter constant (Fig. 2B). At a given speed, larger droplets tended to facilitate particle extraction, and larger amount of MPs tended to promote droplet dispensing. This can be explained by the fact that, with all else constant, friction increases with droplet volume, thus causing NP2 to yield first;  $F_m$  increases with MPs amount, thus causing NP1 to yield first. To visualize these results, we have constructed a 3D phase diagram by summarizing our observations (Fig. 2C and supporting information Fig. S3).

The additional force provided by the SETs enables unique droplet operations on the SETs magnetic droplet platform. In particular, SETs allow liquid dispensing, thereby providing a full range fluidic operations and greatly extending the applicability of magnetic droplet systems.

SETs of diverse sizes and functions were arranged on a fully integrated device capable of sample-to-answer, multiplexed genetic detection, from crude samples. Each SET on the device held a specific buffer for the assay, and MPs were used to transfer and combine materials and reagents.

Here we demonstrate the entire process using food color to aid visualization (Fig. 3 and supporting information Video V4). There were a total of 3 stages involved. First, the platform isolated DNA from whole blood using MPs-based solid phase extraction (Fig. 3A and B). Second, the isolated DNA was dispensed into multiple aliquots using SETs (Fig. 3C). Last, DNA aliquots were mixed with droplets containing gene-specific PCR reagents, and the reaction droplets were subjected to thermal cycling (Fig. 3D–F).

In the first stage, buffers required for DNA isolation, including the lysis/binding buffer and washing buffers, were held in position by 4 large SETs on the right side of the chip (Fig. 3A). Whole human blood was incubated with the silica coated MPs and lysis/binding buffer, in which cells were lysed, and DNA adsorbed onto the silica surface. After incubation, MPs were extracted from the lysis/binding buffer droplet with the assistance of SETs (Fig. 3B). MPs were then moved through washing buffer A droplet to remove any carryover contaminants. After that, MPs moved through two other washing buffer droplets in a similar fashion, for further rinsing (Fig. 3B). The 4 SETs-immobilized buffer droplets facilitated MPs extraction, thus greatly improving the performance of DNA extraction on the magnetic droplet platform.

In the second stage, the MPs with surface-bound DNA were incubated with the elution buffer, and the DNA molecules detached from MPs. To detect multiple biomarkers, the eluent containing isolated DNA was split into three aliquots by moving the droplet with MPs over three small SETs (Fig. 3C).

Last, three smaller PCR buffer droplets, each containing a pair of unique primers specific to a different biomarker, were driven by MPs to merge with the three aliquots (Fig. 3D). Subsequently, MPs were removed from the mixture droplets which were held in place by the large SETs (Fig. 3E). The three reaction mixture droplets on the left side of the chip were then placed on a commercial flatbed thermal cycler and subjected to thermal cycling for PCR (Fig. 3F).

The SETs-enabled droplet PCR was monitored in real time using a customized, miniaturized, fluorescence detection system. The detector of the optical system uses a lock-in configuration that allows fluorescence to be measured in ambient light (supporting information Fig. S4). We used the portable optical system for real time PCR detection of the genetic biomarker *RSF1*, after performing DNA extraction from whole blood. We successfully identified *RSF1* in the blood sample, but not in the no-template control (NTC) (Fig. 3G). Multiplexed biomarker detection was achieved by fluorescence scan, which showed stronger signals in human whole blood than in NTC, indicating successful identification of all three genes (*TP53*, *HER2* and *RSF1*) in blood samples (Fig. 3H). All primer and probe sequences are provided in supporting information Table S1.

## Conclusions

We have, for the first time, demonstrated a full range of fluidic operations on a magnetic droplet platform which include droplet transport, fusion, particle extraction, and dispensing. The incorporation of SETs provides an additional mechanism that interacts with the magnetic force for more versatile liquid handling. The SETs anchor the droplet and compete with MPs over the control of the droplet. The SETs enabled magnetic droplet platform takes the advantage of this interaction, and offers a full range of fluidic operations that traditional magnetic droplet platform cannot handle.

In summary, SETs enable a simple and cost-effective microfluidic platform that is able to translate all of the liquid operations required for assay preparation into the droplet format,

thus allowing complex tasks with microliter volumes, and providing a versatile system for portable bioassays. With SETs, we have developed several droplet assay platforms with functions that may not be realized with traditional droplet systems. We advocate that SETs can significantly enhance the functionality, and broaden the applicability, of magnetic droplet platforms to numerous fields of life science.

## Experimental

### SU8 shadow masks fabrication and SETs patterning

The detailed fabrication steps are listed in supporting information.

### Droplet manipulation on SETs-enabled platform

MPs (MagAttract Suspension G, Qiagen) were washed with water, dried, and added to droplets as the motion actuator. The density of the MPs was estimated by measuring the dried weight of particle suspension (200  $\mu$ L). An N52 grade cylindrical neodymium permanent magnet (Diameter $\times$ Length=3/8"  $\times$  1/4") was placed beneath the substrate for MPs actuation. The permanent magnet was either controlled manually or by a motorized translational stage. Detailed operation conditions for each experiment are listed in supporting information.

### Estimating droplet volume dispensed by SETs

Droplets containing fluorescein (100 nM) were dispensed by SETs from the stock droplet. Water (10  $\mu$ L) was added to each dispensed daughter droplet. The volumes of the daughter droplets dispensed by SETs were calculated based on the relative change in fluorescent intensities according to Equation 1.

$$V_d = \frac{C_f}{C_i - C_f} V_{H_2O} \quad (1)$$

Where  $C_i$  and  $C_f$  are the initial and final fluorescein concentrations respectively measured by fluorescent intensities,  $V_d$  is the volume of the daughter droplet and  $V_{H_2O}$  is the volume of water added.

### SETs-enabled integrated sample preparation and genetic detection

Buffers and MPs for DNA extraction is purchased from Qiagen. PCR reagent, primers sequence, and thermal cycling conditions are listed in the supporting information.

## Supplementary Material

Refer to Web version on PubMed Central for supplementary material.

## Acknowledgments

Authors would like to thank the National Institutes of Health (R01CA155305, U54CA151838, R21CA173390) and National Science Foundation (0546012, 1033744) for funding.

## References

1. Daw R, Finkelstein J. *Nature*. 2006; 442:367.
2. deMello AJ. *Nature*. 2006; 442:394. [PubMed: 16871207]
3. El-Ali J, Sorger PK, Jensen KF. *Nature*. 2006; 442:403. [PubMed: 16871208]
4. Janasek D, Franzke J, Manz A. *Nature*. 2006; 442:374. [PubMed: 16871204]
5. Yager P, Edwards T, Fu E, Helton K, Nelson K, Tam MR, Weigl BH. *Nature*. 2006; 442:412. [PubMed: 16871209]
6. Abdelgawad M, Wheeler AR. *Advanced Materials*. 2009; 21:920.
7. Fair RB. *Microfluidics and Nanofluidics*. 2007; 3:245.
8. Pollack MG, Parnula VK, Srinivasan V, Eckhardt AE. *Expert Review of Molecular Diagnostics*. 2011; 11:393. [PubMed: 21545257]
9. Cho SK, Moon H. *Biochip Journal*. 2008; 2:79.
10. Barbulovic-Nad I, Au SH, Wheeler AR. *Lab on a Chip*. 2010; 10:1536. [PubMed: 20393662]
11. Cho SK, Moon HJ, Kim CJ. *Journal of Microelectromechanical Systems*. 2003; 12:70.
12. Lee J, Moon H, Fowler J, Schoellhammer T, Kim CJ. *Sensors and Actuators a-Physical*. 2002; 95:259.
13. Pollack MG, Fair RB, Shenderov AD. *Applied Physics Letters*. 2000; 77:1725.
14. Sista R, Hua Z, Thwar P, Sudarsan A, Srinivasan V, Eckhardt A, Pollack M, Pamula V. *Lab on a Chip*. 2008; 8:2091. [PubMed: 19023472]
15. Pippier J, Inoue M, Ng LFP, Neuzil P, Zhang Y, Novak L. *Nature Medicine*. 2007; 13:1259.
16. Pippier J, Zhang Y, Neuzil P, Hsieh TM. *Angewandte Chemie-International Edition*. 2008; 47:3900.
17. Zhang Y, Park S, Liu K, Tsuan J, Yang S, Wang TH. *Lab on a Chip*. 2011; 11:398. [PubMed: 21046055]
18. Rida A, Fernandez V, Gijs MAM. *Applied Physics Letters*. 2003; 83:2396.
19. Chiou PY, Ohta AT, Wu MC. *Nature*. 2005; 436:370. [PubMed: 16034413]
20. Baigl D. *Lab on a Chip*. 2012; 12:3637. [PubMed: 22864577]
21. Park S, Chiou PY. *Advances in Optoelectronics*. 2011; 2011:909174.
22. Guttenberg Z, Muller H, Habermuller H, Geisbauer A, Pippier J, Felbel J, Kielpinski M, Scriba J, Wixforth A. *Lab on a Chip*. 2005; 5:308. [PubMed: 15726207]
23. Fan SK, Hsieh TH, Lin DY. *Lab on a Chip*. 2009; 9:1236. [PubMed: 19370242]
24. Wang Y, Zhao Y, Cho SK. *Journal of Micromechanics and Microengineering*. 2007; 17:2148.
25. Zhao Y, Yi UC, Cho SK. *Journal of Microelectromechanical Systems*. 2007; 16:1472.
26. Ng AHC, Choi K, Luoma RP, Robinson JM, Wheeler AR. *Analytical Chemistry*. 2012; 84:8805. [PubMed: 23013543]
27. Yang H, Mudrik JM, Jebraill MJ, Wheeler AR. *Analytical Chemistry*. 2011; 83:3824. [PubMed: 21524096]
28. Sista RS, Eckhardt AE, Srinivasan V, Pollack MG, Palanki S, Pamula VK. *Lab on a Chip*. 2008; 8:2188. [PubMed: 19023486]
29. Eydelnant IA, Uddayasankar U, Li BB, Liao MW, Wheeler AR. *Lab on a Chip*. 2012; 12:750. [PubMed: 22179581]
30. Fiddes LK, Luk VN, Au SH, Ng AHC, Luk V, Kumacheva E, Wheeler AR. *Biomicrofluidics*. 2012; 6
31. Witters D, Vergauwe N, Vermeir S, Ceysens F, Liekens S, Puers R, Lammertyn J. *Lab on a Chip*. 2011; 11:2790. [PubMed: 21720645]
32. Cho CC, Wallace RM, Filessesler LA. *Journal of Electronic Materials*. 1994; 23:827.
33. Junkin M, Watson J, Geest JPV, Wong PK. *Advanced Materials*. 2009; 21:1247.
34. Uhrich KE, Langowski BA. *Abstracts of Papers of the American Chemical Society*. 2006; 231
35. Rhee SW, Taylor AM, Tu CH, Cribbs DH, Cotman CW, Jeon NL. *Lab on a Chip*. 2005; 5:102. [PubMed: 15616747]

36. Tourovskaia A, Barber T, Wickes BT, Hirdes D, Grin B, Castner DG, Healy KE, Folch A. *Langmuir*. 2003; 19:4754.
37. Long Z, Shetty AM, Solomon MJ, Larson RG. *Lab on a Chip*. 2009; 9
38. Shikida M, Takayanagi K, Inouchi K, Honda H, Sato K. *Sensors and Actuators B: Chemical*. 2006; 113:563.

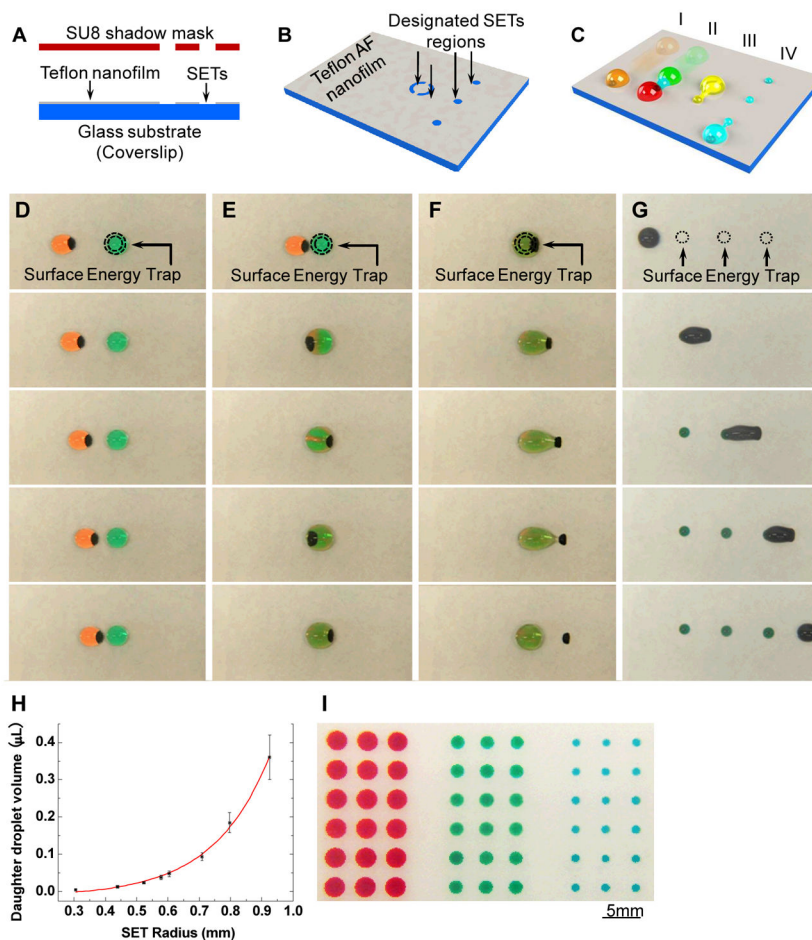


**Figure 1.**

Droplet Operations with SETs. (A) The shadow mask made of SU8 photoresist, lithographically fabricated by a lift-off process, is used to pattern SETs on the Teflon-coated glass substrate. (B) SETs are patterned by selectively etching the Teflon AF film with  $O_2$  plasma passing through perforations in the SU8 shadow mask. (C) The Teflon AF film provides a low energy surface for (I) droplet transport and (II) droplet fusion. SETs are used to (III) pin down the contact line for extraction of MPs from the droplet and (IV) to withhold portions of the liquid to generate new daughter droplets. (D–G) Full-range droplet manipulation on a glass substrate with SETs is achieved on SETs enabled droplet platform. MPs are shown in black. (D) Droplet transport. (E) Droplets fusion and mixing. The MPs oscillate in the fused droplet, thus speeding up mixing. (F) MPs extraction. (G) Droplets dispensing. Compared to droplet and MPs size, SETs are not large enough to trap the entire droplets, and thus only a small portion of the liquid is held back by each SET. (H) Liquid dispensing using SETs. The volume dispensed by SETs is determined by size of SETs. For droplets generated on the same chip with SETs of the same size, the coefficient of variation (CV) in volume was approximately 3% (supporting information Fig. S2). For droplets dispensed on different chips, the CV was larger, approximately 10%, due to chip-to-chip variation. (I) Droplet microarray generated using 3 different sizes of SETs.

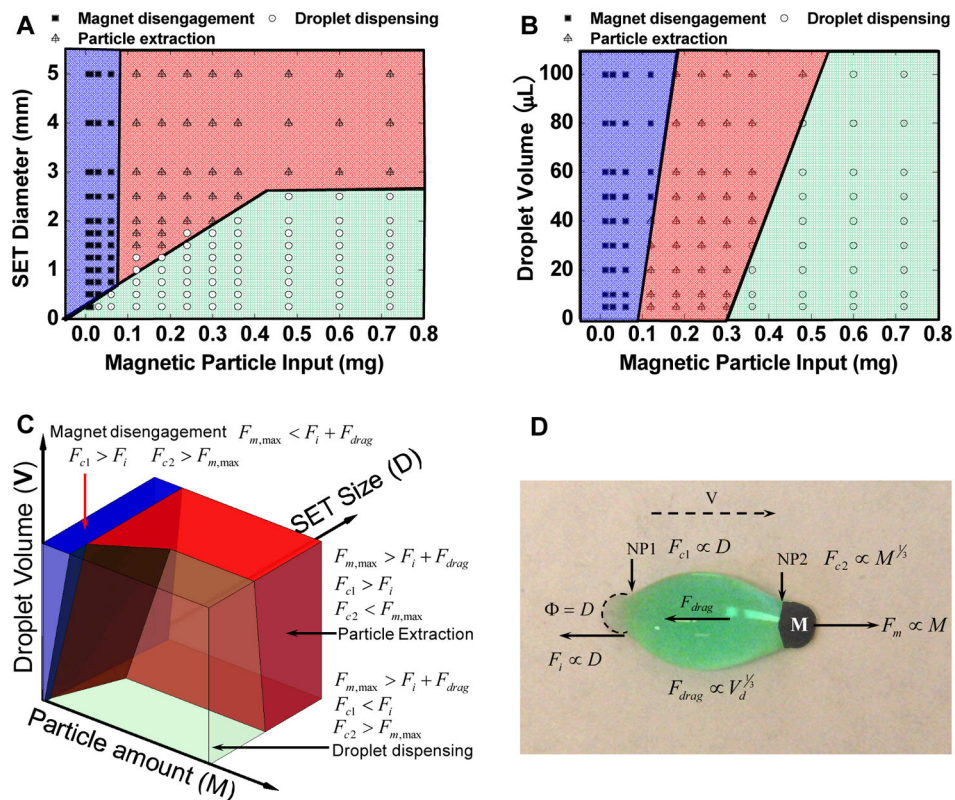


**Figure 2.**

(A) SETs operation phase diagram with constant droplet volume (10  $\mu\text{L}$ ), and variations in magnetic particle input and SET diameter. (B) SETs operation phase diagram with constant SET size (2 mm diameter), and variation in magnetic particle input and droplet volume. (C) 3D phase diagram of SETs enabled magnetic droplet operation (constructed based on the data shown in supporting information Figure S3). (D) Force diagram of the droplet being stretched by the MPs moving over the SETs.

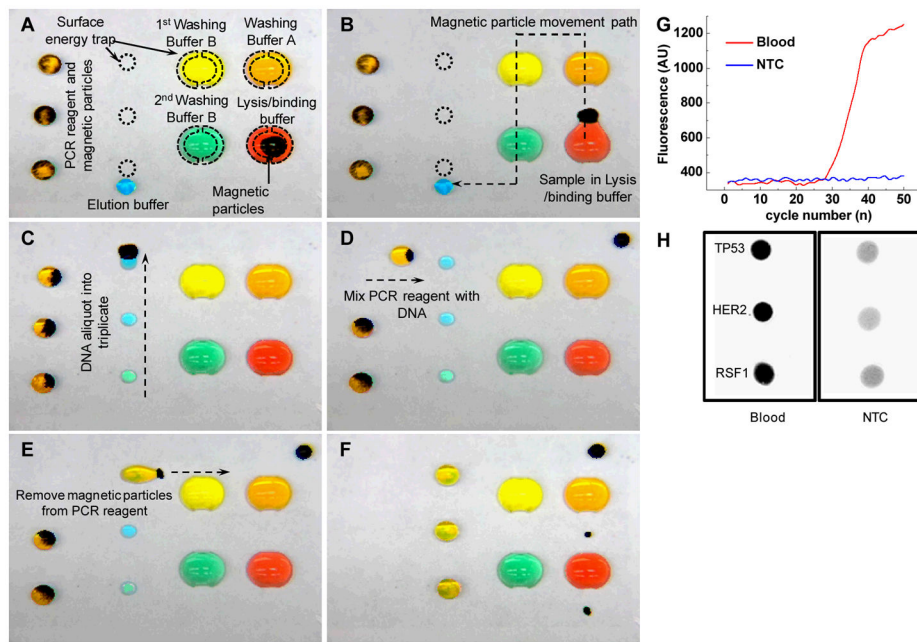


**Figure 3.** Integrated platform for multiplexed genetic detection on a SETs-enabled magnetic droplet platform. (A) The layout of chip with buffers pre-deposited on the designated locations. (B) The crude sample is first mixed with the lysis/binding buffer droplet and MPs (Not shown here). The SETs assist the MPs extraction from the lysis/binding buffer droplet. MPs move through washing buffer droplets to rinse off the contaminants. (C) The eluent containing DNA molecules are made into 3 aliquots by SETs. (D) The PCR reagent droplet is merged with the eluent aliquot. (E) The SETs assist the extraction of the MPs from the reaction mixture. (F) Samples are ready for PCR. (G) Real time amplification curve of PCR on the SETs-enabled droplet platform monitored with customized miniaturized optical detection system (Supporting Information Fig. S4). (H) Multiplexed detection of *TP53*, *HER2* and *RSF1* genetic biomarkers on the SETs-enabled droplet platform. Dark spots indicate positive amplification.